American Journal of Pathology, Vol. 149, No. 2, August 1996

Ultrastructural Instability of Paired Helical Filaments from Corticobasal Degeneration as Examined by Scanning Transmission Electron Microscopy

Hanna Ksiezak-Reding,* Elizabeth Tracz,* Liang-sheng Yang,* Dennis W. Dickson,* Martha Simon,† and Joseph S. Wall†

From the Department of Pathology, Albert Einstein College of Medicine, Bronx, New York, and the Biology Department,† Brookhaven National Laboratory, Upton, Long Island, New York*

Paired helical filaments (PHFs) accumulate in the brains of subjects affected with Alzheimer's disease (AD) and certain other neurodegenerative disorders, including corticobasal degeneration (CBD). Electron microscope studies have shown that PHFs from CBD differ from those of AD by being wider and having a longer periodicity of the helical twist. Moreover, PHFs from CBD have been shown to be primarily composed of two rather than three highly phosphorylated polypeptides of tau (PHF-tau), with these polypeptides expressing no exons 3 and 10. To further explore the relationship between the heterogeneity of PHF-tau and the appearance of abnormal filaments, the ultrastructure and physical parameters such as mass per unit length and dimensions were compared in filaments from CBD and AD using high resolution scanning transmission electron microscopy (STEM). Filament-enriched fractions were isolated as Sarcosyl-insoluble pellets and for STEM studies, samples were freeze-dried without prior fixation or staining. Ultrastructurally, PHFs from CBD were shown to be a heterogeneous population as double- and single-stranded filaments could be identified based on their width and physical mass per unit length expressed in kilodaltons (kd) per nanometer (nm). Less abundant, double-stranded filaments had a maximal width of 29 nm and a mass per unit length of 133 kd/nm, whereas three times more abundant single-stranded filaments were 15 nm wide and had a mass per unit length of 62 kd/nm. Double-stranded filaments also displayed a distinct axial region of less dense mass, which appeared to divide the PHFs into two protofilament-like strands. Furthermore, these filaments were frequently observed to physically separate along the long axis into two single strands or to break longitudinally. In contrast, PHFs from AD were ultrastructurally stable and uniform both in their width (22 nm) and physical mass per unit length (104 kd/nm). The ultrastructural features indicate that filaments of CBD and AD differ both in stability and packing of tau and that CBD filaments, composed of two distinct protofilaments, are more labile under STEM conditions. As fixed and stained filaments from CBD have been shown to be stable and uniform in size by conventional transmission electron microscopy, STEM studies may be particularly suitable for detecting instability of unstained and unfixed filaments. The results also suggest that molecular heterogeneity and/or post-translational modifications of tau may strongly influence the morphology and stability of abnormal filaments. (Am J Pathol 1996, 149:639–651)

In Alzheimer's disease (AD)[1,2] and certain other neurodegenerative disorders, including corticobasal degeneration (CBD),[3,4] progressive supranuclear

Supported by National Institutes of Health grant NS30027 (H. Ksiezak-Reding); Brookhaven STEM United States Department of Energy, Office of Health and Environmental Research; and the National Institutes of Health Biotechnology Resources RR 01777 (J. S. Wall).

Accepted for publication March 29, 1996.

Address reprint requests to Dr. Hanna Ksiezak-Reding, Department of Pathology, Room F-538, Albert Einstein College of Medicine, 1300 Morris Park Avenue, Bronx, NY 10461.

palsy (PSP),[5,6] and Pick's disease,[7,8] highly phosphorylated tau proteins accumulate in brain tissue in association with abnormal filaments. These filaments are the primary component of many pathological inclusions including neurofibrillary tangles, Pick bodies, neuropil threads, and neurites in senile plaques, which are characteristically detected in some of these disorders.[9–13] Ultrastructurally, the abnormal tau-immunoreactive filaments have characteristics unique to each disease, but they can essentially be categorized into two groups of either straight or twisted filaments, depending on whether their width remains constant along the length of the filament or changes periodically. Paired helical filaments (PHFs) of AD were the first twisted filaments described and named by Michael Kidd in 1963.[14] In some of the disorders, only one kind of filament predominates, eg, straight filaments in PSP[15] or twisted filaments in AD[1,2] and CBD.[3] In others, for example, in Pick's disease, both straight and twisted filaments can clearly be distinguished.[16] The unique appearance of filaments also depends on their width, which may vary in straight filaments from 12 to 18 nm (Pick's disease)[16–18] or 12 to 16 nm (PSP).[19] With twisted filaments, however, the width is generally larger and at the maximum may attain 20 to 26 nm (AD),[20,21] 24 nm (Pick's disease),[22] or 26 to 28 nm (CBD).[3] As tau is the major component of various abnormal filaments, their unique ultrastructural features may result from heterogeneity of tau isoforms and/or differential packing of the tau protein. In normal human brain, six different isoforms of tau have been demonstrated in adult subjects, which vary in the expression of exons 2, 3, and 10.[23,24] The expression of these exons is developmentally regulated; in fetal human brain, only one isoform of tau lacking expression of exons 2, 3, and 10 has been described.[24,25] Additional microheterogeneity is reflected in the phosphorylation state of tau.[26] Tau with a high degree of phosphorylation, resembling that of PHF-tau, has recently been detected in biopsy samples of human brain as well as in rodents,[27] suggesting that phosphorylation may have an important role in functioning of tau as a microtubule-associated protein.[28] In AD, abnormal filaments contain three highly phosphorylated polypeptides of tau (PHF-tau) as demonstrated by sodium dodecyl sulfate (SDS)-polyacrylamide gel electrophoresis and direct phosphate analysis.[2,29] Although up to six polypeptides of PHF-tau can be distinguished after dephosphorylation,[30,31] the isoform composition of PHF-tau differs from that of normal tau due to the greatly diminished expression of exon 10.[32] In other neurodegenerative disorders, the isoform composition of tau incorporated into abnormal filaments has only recently been examined. For example, in CBD, in contrast to AD, our studies have demonstrated the lack of expression of exons 3 and 10, whereas in PSP, exon 3 was found to be expressed.[3,33] The results of these studies strongly suggest that abnormal filaments specific for each of the disorders are composed of a unique pattern of PHF-tau isoforms, which may be responsible for the characteristic ultrastructural feature of these filaments.

The packing arrangement of tau molecules in filaments is uncertain. In particular, it is unclear whether PHFs are formed from two or more protofilaments.[34,35] PHFs of AD appear to be composed of paired filaments twisted every 70 to 90 nm or double-stranded twisted ribbons.[20] Although the axial region between the two strands can easily be detected with a variety of negative and positive staining reagents, it is uncertain whether the middle region between the two strands represents staining artifact due to the increased dye binding or is an integral ultrastructural feature of PHFs representing a separation or cleft between the two strands. Images of unstained and unfixed PHFs obtained by either scanning transmission electron microscopy (STEM)[21] or atomic force microscopy[36] or by using platinum-carbon replicas[37] have no distinct two-stranded appearance, suggesting that the axial region of PHFs is an artifact of staining and/or fixation.

PHFs in isolated preparations from CBD brains have recently been examined by conventional EM, and their ultrastructure was reported to differ from that in AD.[3] They were not only 10 to 20% wider in their maximal and minimal widths but also twisted at much longer 200-nm intervals. Furthermore, uranyl-acetate-stained filaments from CBD have a very prominent axial region. The double-stranded appearance of these filaments is more pronounced than that observed in AD. The filaments from CBD have not previously been examined by STEM, and it is uncertain whether the presence of the axial region can be demonstrated for these filaments.

In addition to revealing at high resolution (1 to 2 nm) the ultrastructural details of various PHFs, the STEM technique accurately determines the distribution of physical mass along the length of filaments.[38] For example, in PHF-enriched fractions from AD, our studies have demonstrated the existence of two populations of filaments with the distribution of mass per unit length in the range of 107 to 120 kd/nm and 79 to 85 kd/nm.[21] The differences in mass per unit length between the two populations correlated well with the presence or absence of certain tau epitopes and with changes in their physical dimensions, pos-

sibly the result of proteolytic degradation of some of the filaments in AD.[39] Differences in ultrastructural appearance of PHFs from AD and CBD as well as in the isoform composition of PHF-tau strongly suggest that the arrangement of tau molecules differs between the two kinds of filaments.

In the present comparative studies, the ultrastructure and physical mass per unit length of filaments from both CBD and AD were examined by STEM. We have found that filaments from CBD, unlike PHFs from AD, were diverse in their ultrastructure. Two subpopulations of either double- or single-stranded filaments could be distinguished depending upon mass per unit length and maximal width. Moreover, in some of the filaments, two protofilament-like strands were observed to partially separate and break off, suggesting that filaments from CBD are structurally highly unstable.

Materials and Methods

Tissues

Brain tissue from two subjects with CBD, two subjects with AD, and one aborted fetus were used for our studies. The brain tissue from both CBD subjects has also been used in our previous studies[3]; case 1 was a 71-year-old woman (6-hour postmortem delay), and case 2 was a 74-year-old woman (24-hour postmortem delay). The diagnosis of CBD was based on pathological findings of neuronal loss in cortex and substantia nigra and ballooned neurons in cortex, basal ganglia, and brainstem. AD subjects included case 3, an 80-year-old man (8-hour postmortem delay), and case 4, a 74-year-old woman (5-hour postmortem delay). The diagnosis of AD was based on modified, age-adjusted criteria of Khachaturian.[40] The number of neurofibrillary tangles in frontal and temporal lobes ranged between 2 and 6 per 40× objective field. Fetal brain was obtained snap-frozen in liquid nitrogen from a 19-week-old gestation age fetus. Brain tissue was stored at −80°C until used.

Isolation of PHFs

PHF-enriched fractions were obtained from frontal and temporal lobes (AD) or parietal and occipital lobes (CBD) by the procedure described previously.[3] In that procedure, Sarcosyl-insoluble 100,000 × *g* pellets were obtained and either used directly for most of the experiments or were subjected to additional purification on sucrose density gradient.[21,39] A 1 mol/L sucrose gradient fraction, which contained an abundance of short and dispersed filaments, was collected.

Normal and Recombinant Tau

Normal tau preparation was obtained from fetal human brain using heat and perchloric acid treatments according to previously described procedures.[29] Recombinant human tau protein was expressed in *Escherichia coli* BL21 (DE3 cells) using an expression plasmid pRK172 containing a tau cDNA (clone htau40) encoding the longest tau isoform of 441 amino acid residues.[23,24]

Antibodies

Alz 50 and PHF-1, two monoclonal tau antibodies that bind to amino- and carboxyl-terminal epitopes of human tau,[41,42] respectively, were kindly provided by Dr. Peter Davies. PHF-1 but not Alz 50 recognizes a phosphorylated epitope. Two antibodies, Ab304 and Ab189, were generated in rabbits using tau synthetic peptides from sequences encoded by exon 2 or exon 3, respectively. These antibodies, a generous gift from Dr. Michel Goedert, have been characterized previously.[31,43] Tau-3 is an antibody raised in our laboratory in rabbits against a tau synthetic peptide (EGAPGKQAAAQPHT), corresponding to amino acid sequence 82 to 95 encoded by exon 3. The amino-terminal cysteine residue was added for conjugation purposes, and keyhole limpet hemocyanin was used as a protein carrier. AT100 is a monoclonal antibody kindly donated by Innogenetics (Ghent, Belgium), raised to a PHF-enriched fraction from AD and recognizing a yet unknown phosphorylated epitope in tau.[44]

Gel Electrophoresis and Immunoblotting

Various PHF and tau preparations were subjected to electrophoresis on 10% polyacrylamide-SDS gels and transferred to nitrocellulose paper. Western blotting was performed according to previously described procedures using the ABC Vectastain kit (Vector Laboratories, Burlingame, CA).[39]

EM

Aliquots of PHF samples (25 to 50 μl) were deposited for 5 minutes on copper grids (200 mesh) precoated with Formvar and carbon (E. Fullam, Latham, NY). Grids were washed briefly in phosphate-buffered saline, drained on filter paper, and stained for 5 minutes in a freshly made solution of 2% uranyl ac-

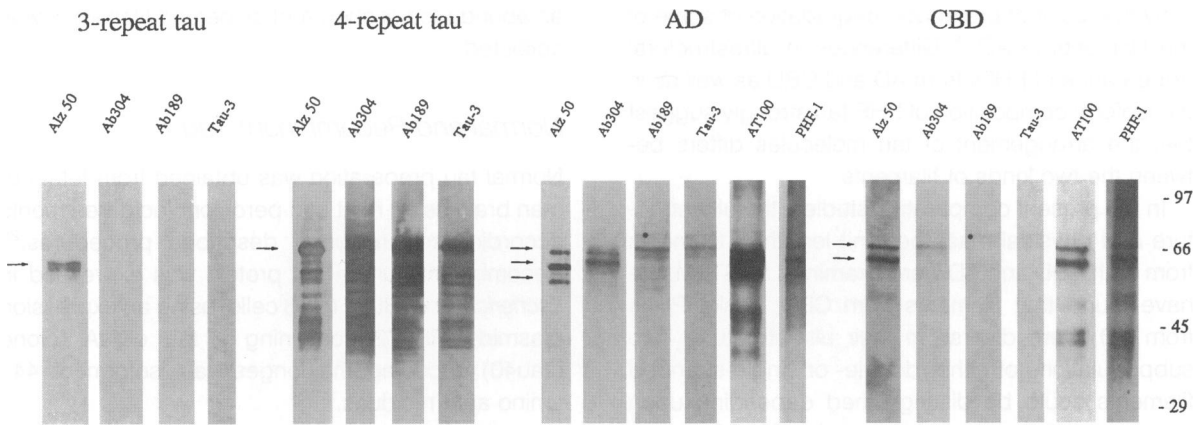

Figure 1. *Immunoreactivity of PHF-enriched fractions from CBD and AD and normal tau with tau antibodies: Western blotting. Tau fraction from human fetal brain* (3-repeat tau), *recombinant tau of the longest isoform* (4-repeat tau), *and PHF-enriched fraction from AD or CBD were immunoblotted with Alz 50, Ab304, Ab189, Tau-3, AT100, or PHF-1 as indicated. Note that only Alz 50 recognized an epitope common to all isoforms of tau (marked with* **arrows**) *including the 55-kd polypeptide expressed in fetal brain, 68-kd recombinant tau, three polypeptides of PHF-tau in AD, and two polypeptides of PHF-tau in CBD. Other antibodies show selective binding to those isoforms of normal tau that express exons 2 and 3 sequences; they recognize recombinant tau but do not bind to fetal tau. In PHF-enriched fractions, Ab304 recognizes only 64- and 68-kd polypeptide of PHF-tau from AD and 68-kd polypeptide from CBD, whereas Ab189 and Tau-3 recognize only 68-kd polypeptide from AD and none in CBD. In comparison, PHF-1 and AT100 bind to all polypeptides of PHF-tau in both AD and CBD.* **Dots** *mark the polypeptide of 70 kd, which shows nonspecific staining in most blots.*

etate in distilled water. After a brief, 1- to 2-second wash in distilled water, grids were air dried and examined by EM using JEOL 100 CX or JEOL 100S.

STEM: Mass and Dimensions

Analyses were performed at the Brookhaven National Laboratory (Upton, NY) using a STEM microscope, essentially as previously described.[21,38] Briefly, grids were thin carbon-coated and either not treated or treated briefly with 0.01 to 0.05% SDS to reduce background and then washed extensively. Grids were precoated with an internal mass standard, tobacco mosaic virus, characterized by a mass per unit length of 131 kd/nm. Samples in solutions were then applied on grids. Grids were extensively washed 10 to 20 times with 20 mmol/L ammonium acetate, pH 7.0, and freeze-dried. The digital STEM images were recorded through a VAX computer system. The mass of the filaments in reference to the tobacco mosaic virus was determined by a computerized program developed at the Brookhaven National Laboratory. Determination of mass was performed along the length of the filament and included both regions of minimal and maximal widths. Maximal width of filaments was measured on STEM micrographs using a 10× measuring microscope (Ted Pella, Redding, CA). Statistical analysis of the mass per unit length and dimension measurements was performed using linear regression, correlation coefficient, and Student's *t*-test.[45]

Results

Characterization of Filaments by Western Blotting

Filament-enriched fractions from CBD and AD brain tissue were obtained as Sarcosyl-insoluble pellets and subjected to Western blotting analysis with tau-reactive antibodies. For comparison, fractions of normal tau proteins obtained from human fetal brain and recombinant tau of the longest (adult) human tau isoform were also analyzed by Western blotting. Immunoblotting was performed with Alz 50, Ab304, and Ab189, three well characterized antibodies, which recognize epitopes encoded by exons 1, 2, and 3, respectively, and Tau-3, another antibody generated with a synthetic peptide for tau exon 3. Alz 50 was found to recognize all isoforms of tau and PHF-tau in the fractions examined, including the 55-kd polypeptide of tau (F-tau) expressed in fetal brain, the 68-kd polypeptide of recombinant tau, three PHF-tau polypeptides of 60, 64, and 68 kd from AD brain and two PHF-tau polypeptides of 64 and 68 kd from CBD brain (Figure 1). The pattern of immunostaining with Alz 50 was consistent with that previously demonstrated for the respective tau fractions.[3,41] In contrast, other antibodies were selective in their immunoreactivity and recognized some but not all tau proteins. For example, Ab304 displayed immunoreactivity with recombinant tau, two (64- and 68-kd) of three PHF-tau polypeptides from AD and the 68-kd

but not the 64-kd polypeptide of PHF-tau from CBD, and did not recognize F-tau. Ab189 and Tau-3 labeled only recombinant tau and the 68-kd polypeptide of PHF-tau from AD and displayed either minimal or no immunoreactivity with PHF-tau polypeptides from CBD and F-tau. Judging from the pattern of immunoreactivity, the antibodies specific for exon 3 sequences, Ab189 and Tau-3, demonstrate a similar selectivity toward tau isoforms. The pattern of immunoreactivity of tau was consistent with that previously demonstrated, including lack of expression of exons 2 and 3 in tau from fetal brain,[43] a low level or no expression of exon 3 in PHF-tau from CBD,[3,33] and the expression of these sequences in PHF-tau from AD.[31,32,43] The results of immunoblotting confirmed that, in comparison with AD, abnormal tau from CBD consists of only two rather than three polypeptides of PHF-tau and that these polypeptides express very little if any of exon 3.

In both disorders, all polypeptides of PHF-tau contained similar phosphorylated epitopes as demonstrated with two phosphate-dependent antibodies AT100 and PHF-1 in these studies (Figure 1) and other antibodies, eg, AT8 or Tau-1 after phosphatase treatment, in our previous report.[3] Except for the unknown location of the AT100 binding site, most of the phosphorylated epitopes are found in conserved regions of tau.

Characterization of Filaments by STEM

Axial Region

As examined by STEM, the filament-enriched fractions from CBD displayed PHF-like filaments (Figure 2, A–F). Most of the filaments were twisted and short in length, rarely exceeding two to three twists defined as a region of minimal width. The average distance measured between two twists, corresponding to one-half of the helical twist was approximately 130 to 150 nm, thus double the length observed in AD, which is approximately 70 to 80 nm (Figure 2, G–K). Aggregated clumps of filaments were sparse. These observations are consistent with our previous EM studies of filaments stained with uranyl acetate before examination by a conventional transmission EM.[3]

Closer examination by STEM revealed that some of the CBD filaments exhibit a very prominent axial region, which was detected as an area of a less dense mass. Cleft of the axial region seemingly divided the filament into two protofilament-like strands and produced a very distinct double-stranded appearance (Figure 2, A and C, and Figure 3A). Ultrastructurally, the filaments appeared labile. For instance, filaments were observed in which a short segment of the protofilament was partially broken off (Figure 3B), whereas in others, the protofilaments had physically separated along the long axis into two individual strands, still attached at one end (Figure 3, C and D). As can be readily seen in Figure 3D, these filaments (or protofilaments) remained twisted, although with other single-stranded filaments, the twisting was less noticeable (Figure 2, D and F). In rare cases, entire filaments were broken transversely along the short axis into two partially detached pieces (Figure 3C). In parallel examinations, samples of PHF from AD, although displaying what appeared to be transversely broken filaments (Figure 2K), were devoid of longitudinally separated filaments, suggesting that these filaments were structurally more stable. It was possible that the structural lability of CBD filaments may have resulted from exposure either to Sarcosyl during the isolation procedure, 20 mmol/L ammonium acetate used to wash STEM samples on grids, or the freeze-drying procedure *per se*. As these factors had no effect on the stability of PHF from AD, however, the structural lability was apparently inherent to filaments from CBD.

Physical Mass and Width

STEM examination revealed that, in CBD samples, both individual filaments and frequently distinct regions of the individual filaments appeared to noticeably vary in both the maximal thickness and the physical mass per unit length estimated in kilodaltons per nanometer (Figures 2 and 3). As illustrated in the histogram pooled from two cases (Figure 4A), of a total of 73 filaments examined, two subpopulations of filaments could clearly be distinguished. One subpopulation consisted of 12- to 16-nm-wide filaments, which were observed more frequently ($n = 28$) than filaments from another subpopulation, which was composed primarily of 28- to 32-nm-wide filaments ($n = 12$). Filaments wider than 32 nm or thinner than 12 nm and those of intermediate sizes were also observed, albeit less frequently. In these studies, only the maximal width of filaments was considered since regions of the minimal width, especially in single-stranded filaments, were often too ambiguous or too rare an occurrence to perform a reliable statistical analysis. In double-stranded filaments, the minimal width was approximately one-half of that in the widest region. The physical mass per unit length of filaments in the two cases examined showed an asymmetric distribution as well. The ma-

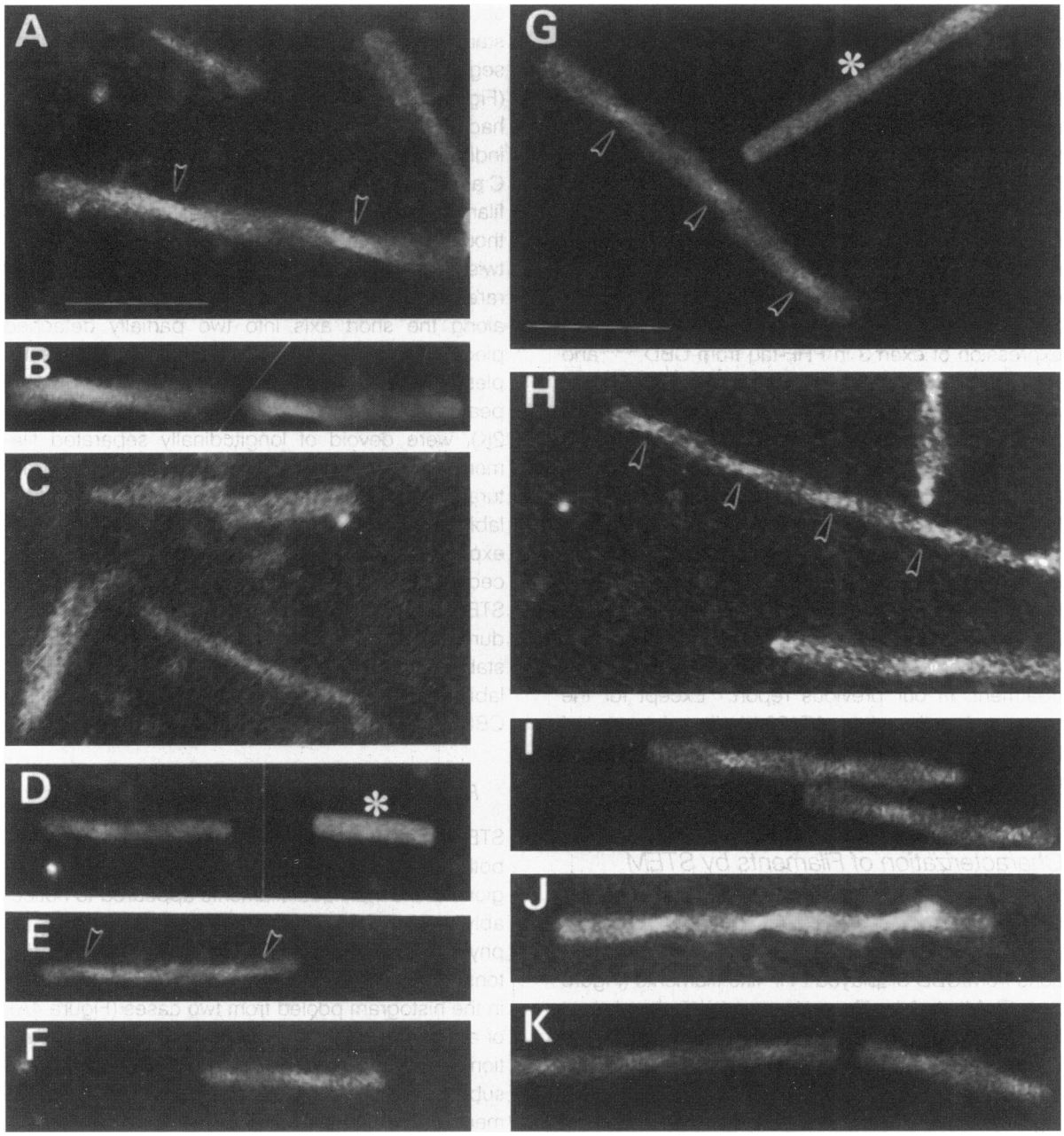

Figure 2. *STEM micrographs of selected filaments from CBD and AD. Samples of PHF-enriched fractions obtained from CBD* (A *to* F) *or AD brains* (G *to* K) *as Sarcosyl-insoluble pellets were deposited on grids precoated with tobacco mosaic virus as a mass standard* (asterisks *in* D *and* G). *The mass of filaments per unit length was compared with that of the standard (131 kd/nm) using a computerized program developed in the Brookhaven National Laboratory. Note that filaments from CBD are twisted approximately every 130 to 150 nm, whereas those from AD are twisted every 70 to 80 nm* (arrowheads) *and that, in contrast to AD, they vary in maximal width. Filaments from CBD are either double stranded with mass per unit length between 95 and 151 kd/nm* (A *to* C) *or single stranded with mass per unit length between 54 and 70 kd/nm* (C *to* F). *Filaments from AD have approximate mass per unit length from 83 kd/nm (middle filament in* H, *and* J) *to 128 kd/nm* (G). *Scale bar, 100 nm.*

jority of filaments were characterized by the mass per unit length of 50 to 75 kd/nm, and these filaments were observed more often (n = 47) than filaments with the mass per unit length higher than 75 kd/nm. Among filaments >75 kd/nm, those with the mass per unit length between 125 and 150 kd/nm were detected somewhat more frequently (n = 13). We were interested to know whether a relationship exists between the mass per unit length and the width of the filaments. Therefore, a histogram of the mass per unit length values was constructed and superimposed on a graph of the width of the respective filaments (Figure 5). The results clearly indicate that filaments characterized by a mass per unit length of

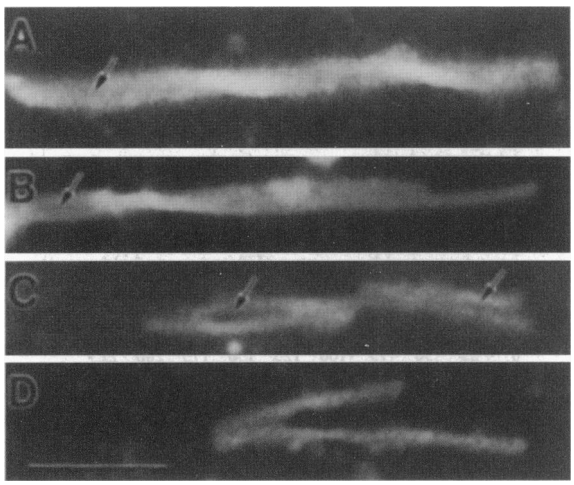

Figure 3. *STEM micrographs of filaments from CBD displaying ultrastructural instability.* A: *The filament has a darker axial region of less dense mass* (arrow) *and appears double stranded; the mass per unit length of the filaments is estimated at approximately 136 kd/nm (n = 12).* B: *The filament with a prominent axial region* (arrow) *and a mass per unit length of 135 kd/nm (n = 14) has a section of strand or protofilament missing at one end and a mass per unit length reduced to 60 kd/nm (n = 4).* C: *The filament either splits longitudinally into two individual strands, which are separated in the middle* (arrows) *but still attached at one end or it breaks transversely into two partially attached fragments.* D: *The double-stranded filament with a mass per unit length of 126 kd/nm (n = 2) has already separated into two individual single-stranded filaments with a mass per unit length of 68 and 69 kd/nm (n = 13), which are still twisted. Scale bar, 100 nm.*

50 to 75 kd/nm were on average 15 nm wide, whereas those with an approximate mass per unit length of 125 to 150 kd/nm were approximately double in size and had a maximal width of approximately 29 nm. Furthermore, although some filaments had a mass per unit length of less than 50 kd/nm or greater than 150 kd/nm, their width remained rather constant at 15 nm or 29 to 32 nm, respectively. Linear regression analysis was performed for the width and mass data (not shown). The existence of a highly significant relationship between the mass per unit length and the width of the filaments was confirmed by a high correlation coefficient of $r = 0.864$ ($P < 0.001$; n = 73).

Interestingly, in samples of PHFs from AD, which were examined in parallel, similar variability in the width (maximum) and the physical mass per unit length was not observed. In two different cases of AD, the width of a total of 55 filaments examined was rather uniform as the majority of filaments (n = 28) were 20 to 24 nm wide (Figure 5C). A histogram of mass values indicates that the majority of filaments (n = 33) were also characterized by a mass per unit length of 100 to 125 kd/nm. A comparison of filaments from both disorders by STEM indicates that only CBD filaments represent a mixed population, consisting of primarily 29-nm- or 15-nm-wide filaments, with an approximate mass per unit length of 133 kd/nm and 62 kd/nm, respectively, and that the 15-nm filaments are three times more abundant (Table 1).

The packing density of tau, defined as mass per nm^3, can be calculated for the filaments based on their mass per unit length and the maximal and minimal widths, assuming that the filament is a ribbon.[20,21] In these calculations, the values for minimal width of double-stranded CBD filaments and AD filaments were supplemented with that reported elsewhere for 49 to 65 measurements.[3] In single-stranded filaments, minimal width values were considered similar to that for double-stranded filaments. The calculated packing density of tau has been found to be somewhat lower in CBD than AD, as the values of 0.31 to 0.34 kd/nm^3 and 0.40 kd/nm^3 were obtained for the respective filaments (Table 1). The differences in packing density between filaments were statistically significant ($P < 0.001$). The number of tau molecules per unit length of filament can also be calculated as the molecular mass of tau is known. For CBD filaments, assuming a molecular mass of 38.3 kd (average of two isoforms of 352 and 381 amino acid residues) and a 3-nm length proposed for axial spacing in the model of PHF,[20] an estimated 4.9 and 10.5 molecules of tau are packed in a single- or double-stranded filament, respectively. For PHFs from AD and the molecular weight of tau set at 41.3 kd (average of all six isoforms), 7.6 molecules per 3-nm length are estimated, and this value is consistent with that of 8.4 previously reported.[21]

Discussion

The results of the present study demonstrate that PHFs from CBD and AD differ in both biochemical composition as well as ultrastructural morphology. When examined by STEM, filaments from CBD appear to be ultrastructurally unstable and heterogeneous in both maximal width and physical mass per unit length. By immunoblotting, PHF-enriched fractions from CBD display a reduced number of PHF-tau polypeptides, which lack expression of certain adult-specific epitopes. It is very likely that specific ultrastructural characteristics and compromised stability of these filaments are related to their unique biochemical composition.

CBD: Single- and Double-Stranded Filaments

In the present study, ultrastructural heterogeneity of filaments from CBD has been demonstrated by the

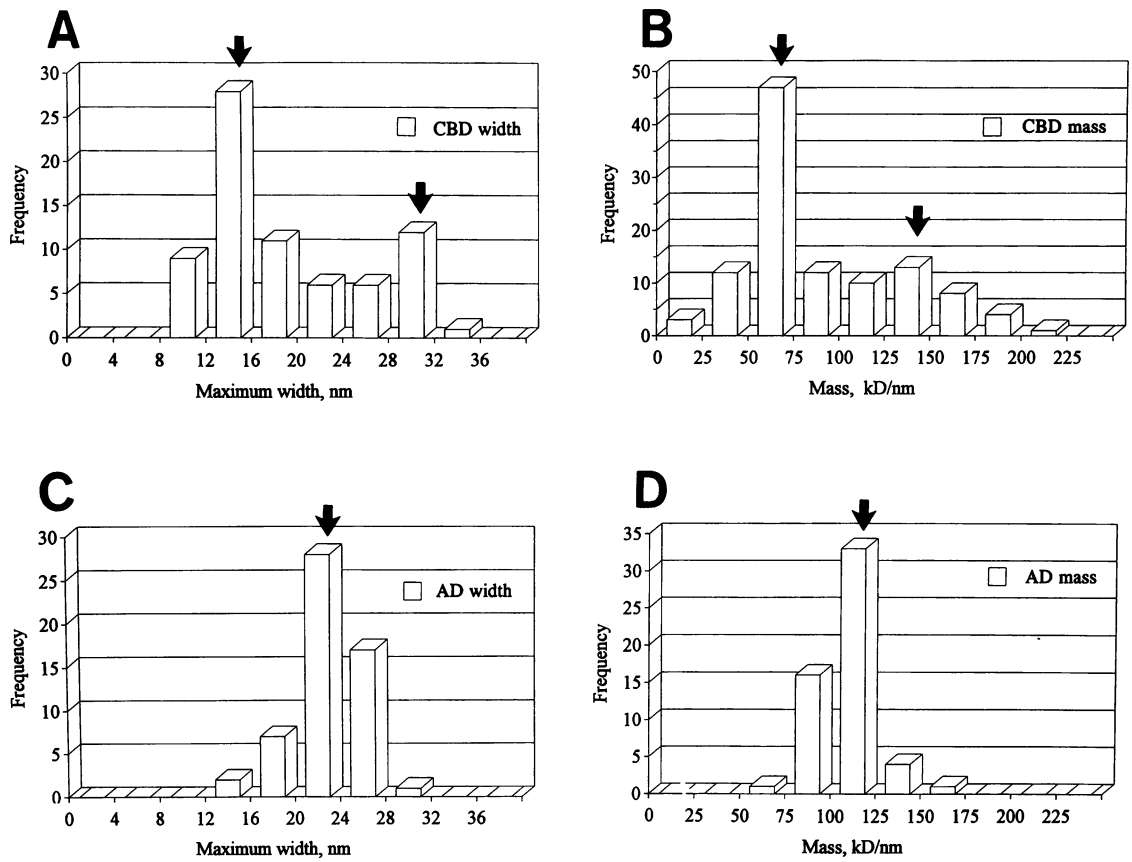

Figure 4. *Histogram of maximal width* (A *and* C) *and the mass per unit length of filaments from CBD and AD* (B *and* D, *respectively*). *The width of filaments was determined using STEM micrographs and the values represent the mean for 1 to 5 measurements of 73 filaments* (*CBD, case 1*) *or the mean for 1 to 4 measurements of 55 filaments* (*AD, two cases*). *The mass data were obtained by STEM and represent the mean values for 2 to 12 measurements of 110 filaments* (*CBD, two cases*) *or the mean values for 3 to 17 measurements of 55 filaments* (*AD, two cases*). *In CBD, the frequency distribution of the width and the mass per unit length indicate the presence of two subpopulations of filaments* (arrows *in* A *and* B), *whereas in AD, only one population can be distinguished* (arrow *in* C *and* D).

presence of two distinct subpopulations of filaments, distinguished by their different maximal width and mass per unit length. Although one subpopulation contained 15-nm-wide filaments with an average mass per unit length of 62 kd/nm, another subpopulation contained wider filaments (29 nm) and with greater mass per unit length (133 kd/nm). The comparison of both parameters suggests that the 15-nm filaments could originate from the 29-nm filaments simply by separation of fibrils along the long axis. Indeed, the axial region, which was recognized as a region containing less dense mass was very distinct in the 29-nm filaments. The presence of a distinct cleft in the axial region lends a double-stranded appearance to these filaments even before the two strands actually separate, suggesting that such a feature may be an attribute of filaments, which are ultrastructurally unstable. Furthermore, in the STEM micrographs, the process of separation of the 29-nm-wide filament into two components could be observed in a step-like fashion. Judging from the frequency distribution, only approximately 25% of the total population from CBD were approximately 29-nm-wide filaments, suggesting that most of the filaments have already separated into smaller size components. Therefore, the process of separation into

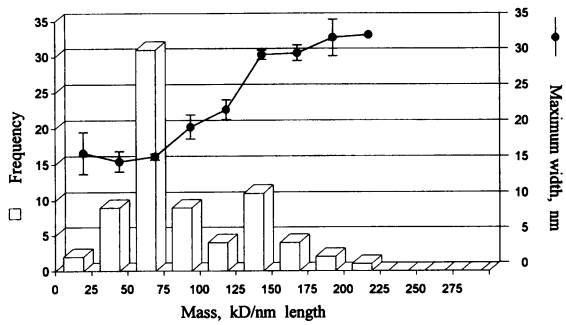

Figure 5. *The relationship between mass per unit length and maximal width of the filaments from CBD. Histogram of the mass per unit length was superimposed with the width of the respective filaments* (*n = 73; case 1*). *In the graph, values are means ± SD or ± range for 1 to 31 filaments. The combination histogram/graph clearly shows that filaments low in mass per unit length* (*range, 0 to 75 kd/nm*) *are 15 nm wide and filaments with more mass per unit length* (*range, 125 to 225 kd/nm*) *are approximately 30 nm wide.*

Table 1. *Physical Mass per Unit Length and Maximal Width of Filaments from CBD and AD and the Calculated Values for Packing of tau*

Type of Filament	Mass (kd/nm length)	Maximal width (nm)	Mass density (kd/nm^3)	Mass (kd/3-nm length)	Tau molecules/ 3-nm length
CBD, single stranded*	62 ± 7.4 (47)	15 ± 2.4 (31)	0.31 ± 0.037 (47)	186 ± 22 (47)	4.9 ± 0.6 (47)
CBD, double stranded*	133 ± 6.6 (13)	29 ± 2.1 (11)	0.34 ± 0.017 (13)	399 ± 20 (13)	10.4 ± 0.5 (13)
AD, total	104 ± 14.3 (55)	22 ± 3.0 (55)	0.40 ± 0.055 (55)	313 ± 43 (55)	7.6 ± 1.0 (55)

Physical mass per unit length and maximal width of filaments from CBD and AD, isolated as Sarcosyl-insoluble pellets (see Materials and Methods), were determined by STEM and using STEM micrographs, respectively. For CBD, the results are selected from data in Figures 4 and 5 and represent values for the most frequent ranges of filaments (CBD, single or double stranded). For comparison, values for the total population of PHF from AD are presented (AD, total). Values are means ± SD for the number of filaments in the parentheses. Mass density was calculated based on the values for maximal width obtained in the present studies and the minimal width of 13.5 or 11.5 nm for CBD and AD filaments, respectively, reported elsewhere.[3,21] The number of tau molecules per 3-nm length of filaments was calculated from the values of mass by STEM with the molecular mass of tau set at 41.3 kd (AD; average of all six isoforms) or 38.3 kd (CBD; average of two isoforms of 352 and 381 amino acid residues).

*$P < 0.001$ as compared with AD or other filaments in CBD.

two 15-nm filaments is more than just sporadic in nature. It is possible, however, that the reverse process took place and two single filaments combined to form a double-stranded structure. Results of the present studies cannot always distinguish between these two possibilities (Figure 3D), although a double-to-single transition is evident in most cases (Figure 2, A, B, and top of C, and Figure 3, A–C). Another arrangement, which requires a single filament to bend over to form a double-stranded structure, is less likely to occur since CBD as well as AD filaments appear rigid in their ultrastructure and no serious bending is ever observed.

AD: PHFs

In contrast to CBD filaments, PHFs obtained from AD brain have been demonstrated to be ultrastructurally stable in this study as well as in previous studies using STEM.[21] Except for breaking longitudinally into smaller fragments, no fraying at the ends or separating into two protofilaments along the axis have been observed with these filaments, although these features have been reported by others in some PHFs examined with conventional transmission EM.[20] Moreover, in the present study, the whole population was uniform in size (maximal width of 22 nm) and mass per unit length (104 kd/nm). These values are comparable to that previously described for an SDS-soluble, undigested population of PHFs with maximal width of 22 to 26 nm and mass per unit length of 107 to 120 kd/nm but differ from that described for another population.[21] That population of PHFs was characterized by a smaller average size (16 to 20 nm) and lighter mass per unit length (79 to 85 kd/nm) and was subsequently demonstrated to be composed of proteolytically degraded PHF-tau devoid of amino-terminal tau epitopes.[39] Although it is possible that the PHF fraction examined in the present study contained small amounts of digested filaments, the majority of filaments were intact, composed of full-length PHF-tau molecules, and thus by physical parameters (mass and dimensions) or by morphological or biochemical criteria resembled SDS-soluble and undigested PHFs.[21,39] The possibility that, in CBD, the presence of two populations of filaments could be due to proteolytic degradation is very unlikely. For example, proteolysis could not account for a loss of only one of the paired protofilaments or separation into two individual protofilaments corresponding in the size and mass per unit length to exactly one-half of the parental double-stranded filament. Our results strongly support the hypothesis that structural instability, rather than proteolytic digestion, is involved in the generation of two subpopulations of filaments in CBD.

Filaments in Other Disorders

The presence of two populations of filaments has frequently been demonstrated in some of the neurodegenerative disorders, eg, Pick's disease,[22,46] but less frequently in others, eg, PSP or AD. In Pick bodies, twisted, 24-nm-wide filaments have been observed intermixed with 12- to 18-nm straight filaments.[16–18,22] In PSP, a small number of PHFs has been described to co-exist with narrower, straight filaments.[19,47] In AD, few straight filaments have been detected in the majority of PHFs.[2,48–50] Most interestingly, a concept of the continuous transformation of the cytoskeletal network has been introduced in AD, with the presence of a threshold or phase transition.[51] Such a treshold could correspond to the transition from the single- to double-stranded filaments and support our hypothesis of the precursor/product relationship between straight and

twisted populations of filaments in some of the neurodegenerative disorders. A similar conclusion has been reached by others in EM studies of heterogeneous populations of filaments isolated from Pick bodies.[16,22] Furthermore, it is possible that the wide, double-stranded filaments are less abundant in some of the disorders because of their highly unstable ultrastructure, perhaps even more labile than that in CBD. The ultrastructural stability could then be the primary determinant of whether one or two populations of filaments are formed and/or which of the populations is more abundant. However, the ultrastructural stability of filaments in Pick's disease, PSP, and other disorders is not known. Some of the heterogeneity could also be due to different packing of tau, which has previously been described for straight and twisted filaments in AD by EM image processing.[49]

STEM versus *EM*

According to previous EM studies, which required negative or positive staining reagents and occasionally fixatives, PHFs were reported to be ultrastructurally stable regardless of whether they originated from AD or CBD.[3] In those studies, the axial region had been observed to stain darker than the rest of the filament and appeared to be defined better in samples from CBD. In AD filaments, however, a prominent staining of the axial region has been reported after alkali treatment,[20,52] and the separation of two strands was occasionally observed after treatment with 2% formic acid.[53]

Previous EM examination of filament-enriched fractions from CBD did not reveal the presence of two subpopulations.[3] Measurements of maximal width for a total of 48 filaments stained with uranyl acetate demonstrated a range of values between 26 and 28 ± 3 to 4 nm (mean ± SD) similar to those described for double-stranded filaments in the present paper. The comparison indicates that the majority of previously examined filaments were double stranded and suggests that the conditions used in EM, but not STEM, studies appear to preserve the ultrastructure of 29-nm-wide filaments. On tissue sections, however, both wide PHF-like and 15-nm straight filaments have been demonstrated by others,[4,12,13] underlying wide ultrastructural fluctuations of filaments in CBD. In addition to the ultrastructural instability of filaments *per se*, some of the variability could be due to the effects of extensive tissue processing for histochemistry or immunocytochemistry.

STEM Technique

The potential limitations of STEM in most cases are related to the poor quality of the specimen including a high content of salts. If the effect of salts on mass measurements cannot be corrected with an internal mass standard, such a specimen has to be discarded. Another potentially limiting factor is the freeze-drying procedure, which according to some reports can cause shrinkage of the unusually open structure, for example, in the disassembled particles of adenovirus type 2.[54] The severe shrinkage of these particles has been attributed to the cavities in the base of the structure and lateral movement of protein to fill these cavities. Although shrinkage might have changed the original size of adenovirus particles, its effect on the molecular mass determination was considered insignificant. In our studies, samples were of sufficient purity and the effects of salts were not evident. Moreover, filaments displayed rather compact structure suggesting that lateral movement of protein and disturbances in mass determination can be considered minimal.

The freeze-drying procedure or the media used for preparing and washing the grids could lower the stability of filaments, freeze-drying by the physical force exerted by crystallization of water molecules and 20 mmol/L ammonium acetate either by low ionic strength or direct effect of ions. Sarcosyl used for isolation of filaments was less likely to cause instability as the same detergent-purified fraction appeared rather stable in EM studies. On the other hand, attachment of filaments to grids is *per se* a harsh process, requiring a direct interaction of proteins with the hydrophobic surfaces on the carbon film, and could easily account for some of the instability. It is uncertain which of the above factors are most important for the stability of the filaments from CBD. Although freeze-drying is notorious for protein denaturation, the effect of chemical reagents or the unique susceptibility of filaments to certain reagents, however, cannot be easily overlooked. For example, according to our previous report, filaments from CBD were observed to partially separate into three to four protofilaments after staining with Nanovan.[55] The effect of Nanovan was specific to CBD and was not observed in samples from AD. Additional studies are required to demonstrate which of the factors, mechanical or chemical, are responsible for the destabilization of abnormal filaments in STEM studies and to identify the mechanisms involved.

Molecular Mechanisms

At present, the molecular basis of such instability is unknown. It may be related to the different packing of tau as compared with that of other more stable filaments, eg, PHFs from AD. Double-stranded filaments from CBD displayed 28% higher values for both the mass per unit length and the maximal width as well as a higher estimated number of tau molecules packed in a 3-nm segment (10.4 *versus* 7.6 molecules in AD). The mass density of filaments, however, was 15 to 22% lower in CBD than AD, suggesting that, although more tau is packed in CBD, the packing is less compact. The difference in the packing may be related to the extent of post-translational modifications of tau in CBD, eg, lower level of ubiquitination[4,56–58] or the suggested higher phosphate content.[3] Such comparisons between filaments from neurodegenerative disorders have not yet been performed. It may also be due to the unique biochemical composition of PHF-tau polypeptides, which in CBD do not express exons 3 and 10, according to this and other reports.[3,33] It is of special interest that PHF-tau polypeptides that lack expression of exon 10 contain only one instead of two cysteine residues and that PHF-tau from AD, in contrast to that in CBD, contains a small number of isoforms expressing exon 10.[32] It remains to be proven whether and how the differences in the biochemical composition of PHF from AD and CBD may affect the stability of filaments and whether the number of cysteine residues or the extent of post-translational modifications of PHF-tau isoforms are of particular importance.

Acknowledgments

The authors thank Dr. Michel Goedert for his generous gift of clone htau40 and antibodies Ab189 and Ab304, Dr. Peter Davies for providing antibody Alz 50 and PHF-1, Ms. Beth Lin for her help in preparation of samples for STEM studies and obtaining some negatives, and Innogenetics, Inc., for their generous supply of antibody AT100.

References

1. Grundke-Iqbal I, Iqbal K, Tung YC, Ouinlan M, Wisniewski HM, Binder LI: Abnormal phosphorylation of the microtubule-associated protein tau in Alzheimer cytoskeletal pathology. Proc Natl Acad Sci USA 1986, 83:4913–4917
2. Greenberg SG, Davies P: A preparation of Alzheimer paired helical filaments that displays distinct tau proteins by polyacrylamide gel electrophoresis. Proc Natl Acad Sci USA 1990, 87:5827–5831
3. Ksiezak-Reding H, Morgan K, Weidenheim K, Mattiace LA, Liu WK, Yen SH, Davies P, Dickson DW: Ultrastructure and biochemical composition of paired helical filaments in corticobasal degeneration. Am J Pathol 1994, 145:1496–1508
4. Wakabayashi K, Oyanagi K, Makifuchi T, Ikuta F, Homma A, Homma Y, Horikawa Y, Tokiguchi S: Corticobasal degeneration: etiopathological significance of the cytoskeletal alterations. Acta Neuropathol 1994, 87:545–553
5. Tabaton M, Whitehouse PJ, Perry G, Davies P, Autilio-Gambetti L, Gambetti P: Alz 50 recognizes abnormal filaments in Alzheimer's disease and progressive supranuclear palsy. Ann Neurol 1988, 24:407–413
6. Flament S, Delacourte A, Verny M, Hauw J-J, Javoy-Agid F: Abnormal tau proteins in progressive supranuclear palsy: similarities and differences with the neurofibrillary degeneration of the Alzheimer type. Acta Neuropathol 1991, 81:591–596
7. Pollock NJ, Mirra SS, Binder LI, Hansen LA, Wood JG: Filamentous aggregates in Pick's disease, progressive supranuclear palsy, and Alzheimer's disease show antigenic determinants with microtubule-associated protein, tau. Lancet 1986, 2:1211
8. Murayama S, Mori H, Ihara Y, Tomonaga M: Immunocytochemical and ultrastructural studies of Pick's disease. Ann Neurol 1990, 27:394–405
9. Braak H, Braak E, Grundke-Iqbal I, Iqbal K: Occurrence of neuropil threads in the senile human brain and in Alzheimer's disease: a third location of paired helical filaments outside of neurofibrillary tangles and neuritic plaques. Neurosci Lett 1986, 65:351–355
10. Hauw J-J, Verny M, Delaere P, Cervera P, He Y, Duyckaerts: Constant neurofibrillary changes in the neocortex in progressive supranuclear palsy: basic differences with Alzheimer's disease and aging. Neurosci Lett 1990, 119:182–186
11. Hof PR, Bouras C, Perl DP, Morrison JH: Quantitative neuropathologic analysis of Pick's disease cases: cortical distribution of Pick bodies and coexistence with Alzheimer's disease. Acta Neuropathol 1994, 87:115–124
12. Mori H, Nishimura M, Namba Y, Oda M: Corticobasal degeneration: a disease with widespread appearance of abnormal tau and neurofibrillary tangles, and its relation to progressive supranuclear palsy. Acta Neuropathol 1994, 88:113–121
13. Feany MB, Dickson DW: Widespread cytoskeletal pathology characterizes corticobasal degeneration. Am J Pathol 1995, 146:1388–1396
14. Kidd M: Paired helical filaments in electron microscopy of Alzheimer's disease. Nature 1963, 197:192–193
15. Oyanagi K, Takahashi H, Wakabayashi K, Ikuta F: Large neurons in the neostriatum in Alzheimer's disease and progressive supranuclear palsy: a topographic, histologic, and ultrastructural investigation. Brain Res 1991, 544:221–226

16. Tokutake S, Oyanagi S: Mechanical instability of Pick bodies and their isolation in an intact form using urea solution. Neurosci Lett 1993, 163:15–18
17. Sparkman DR, Johnson SA, Hammon KM, Allison PM, White CL: Isolation of the insoluble straight fibrils of Pick's disease. J Neurol Sci 1987, 80:173–184
18. Kato S, Nakamura H: Presence of two different fibril subtypes in the Pick body: an immunoelectron microscopic study. Acta Neuropathol 1990, 81:125–129
19. Jellinger KA, Bancher C: Neuropathology. Progressive Supranuclear Palsy: Clinical and Research Approaches. Edited by I Litwan, Y Agid. New York, Oxford University Press, 1992, pp 44–88
20. Wischik CM, Crowther RA, Stewart M, Roth M: Subunit structure of paired helical filaments in Alzheimer's disease. J Cell Biol 1985, 100:1905–1912
21. Ksiezak-Reding H, Wall JS: Mass and physical dimensions of two distinct populations of paired helical filaments. Neurobiol Aging 1994, 15:11–19
22. Takauchi S, Hosomi M, Marasigan S, Sato M, Hayashi S, Miyoshi K: An ultrastructural study of Pick bodies. Acta Neuropathol 1984, 64:344–348
23. Goedert M, Spillantini MG, Potier MC, Ulrich J, Crowther RA: Cloning and sequencing of the cDNA encoding an isoform of microtubule-associated protein tau containing four tandem repeats: differential expression of tau protein mRNAs in human brain. EMBO J 1989, 8:393–399
24. Goedert M, Jakes R: Expression of separate isoforms of human tau protein: correlation with the tau pattern in brain and effects on tubulin polymerization. EMBO J 1990, 9:4225–4230
25. Kosik KS, Orecchio LD, Bakalis S, Neve RL: Developmentally regulated expression of specific tau sequences. Neuron 1989, 2:1389–1397
26. Butler M, Shelanski ML: Microheterogeneity of microtubule-associated tau proteins is due to differences in phosphorylation. J Neurochem 1986, 47:1517–1522
27. Matsuo ES, Shin RW, Billingsley ML, Van de Voorde A, O'Connor M, Trojanowski LQ, Lee VMY: Biopsy-derived adult human brain tau is phosphorylated at many of the same sites as Alzheimer's disease paired helical filament tau. Neuron 1994, 13:989–1002
28. Wiche G, Oberkanins C, Himmler A: Molecular structure and function of microtubule-associated proteins. Int Rev Cytol 1991, 124:217–273
29. Ksiezak-Reding H, Liu W-K, Yen S-H: Phosphate analysis and dephosphorylation of modified tau associated with paired helical filaments. Brain Res 1992, 597:209–219
30. Greenberg SG, Davies P, Schein JD, Binder LI: Hydrofluoric acid-treated tau-PHF proteins display the same biochemical properties as normal tau. J Biol Chem 1992, 267:564–569
31. Goedert M, Spillantini MG, Cairns NJ, Crowther RA: Tau proteins of Alzheimer paired helical filaments: abnormal phosphorylation of all six brain isoforms. Neuron 1992, 8:159–168
32. Ksiezak-Reding H, Shafit-Zagardo B, Yen S-H: Differential expression of exons 10 and 11 in normal tau and tau associated with paired helical filaments. J Neurosci Res 1995, 41:583–593
33. Feany MB, Ksiezak-Reding H, Liu W-K, Vincent I, Yen S-H, Dickson DW: Epitope expression and hyperphosphorylation of tau proteins in corticobasal degeneration: differentiation from progressive supranuclear palsy. Acta Neuropathol 1995, 90:37–43
34. Wisniewski HM, Wen GY: Substructure of paired helical filaments from Alzheimer's disease neurofibrillary tangles. Acta Neuropathol 1985, 66:173–176
35. Miyakawa T, Katsuragi S, Araki K, Hashimura T, Kimura T, Kuramoto R: Ultrastructure of neurofibrillary tangles in Alzheimer's disease. Virchows Arch B Cell Pathol 1989, 57:267–273
36. Pollanen MS, Markiewicz P, Bergeron C, Goh MC: Twisted ribbon structure of paired helical filaments revealed by atomic force microscopy. Am J Pathol 1994, 144:869–873
37. Ruben GC, Novak M, Edwards PC, Iqbal K: Alzheimer paired helical filaments, untreated and pronase digested, studied by vertical platinum-carbon replication and high resolution transmission electron microscopy. Brain Res 1995, 675:1–12
38. Wall JS, Hainfeld JF: Mass mapping with the scanning transmission electron microscope. Annu Rev Biophys Chem 1986, 15:355–376
39. Ksiezak-Reding H, Morgan K, Dickson DW: Tau immunoreactivity and SDS solubility of two populations of paired helical filaments that differ in morphology. Brain Res 1994, 649:185–196
40. Khachaturian ZS: Diagnosis of Alzheimer's disease. Arch Neurol 1985, 42:1097–1105
41. Ksiezak-Reding H, Leibowitz RL, Bowser R, Davies P: Binding of Alz 50 depends on Phe^8 in tau synthetic peptides and varies between native and denaturated tau proteins. Brain Res 1995, 697:63–67
42. Otvos L, Feiner L, Lang E, Shendrei GI, Goedert M, Lee VMY: Monoclonal antibody PHF-1 recognizes tau protein phosphorylated at serine residues 396–404. J Neurosci Res 1994, 39:669–673
43. Goedert M, Spillantini MG, Jakes R, Rutherford D, Crowther RA: Multiple isoforms of human microtubule-associated protein tau: sequences and localization in neurofibrillary tangles of Alzheimer's disease. Neuron 1989, 3:519–526
44. Mercken M, Vandermeeren M, Lubke U, Six J, Boons J, Van de Voorde A, Martin J-J, Gheuens J: Monoclonal antibodies with selective specificity for Alzheimer tau are directed against phosphatase-sensitive epitopes. Acta Neuropathol 1992, 84:265–272
45. Zar JH: Biostatistical Analysis, ed 2. Englewood Cliffs, NJ, Prentice Hall, 1984
46. Perry G, Steward D, Friedman R, Manetto V, Autilio-Gambetti L, Gambetti P: Filaments of Pick's bodies contain altered cytoskeletal elements. Am J Pathol 1987, 187:559–568
47. Masliah E, Hensen LA, Quijada S, DeTeresa R, Alford

M, Kauss J, Terry R: Late onset dementia with argyrophilic grains and subcortical tangles or atypical progressive supranuclear palsy? Ann Neurol 1991, 29: 389–396

48. Papasozomenos SC: Tau protein immunoreactivity in dementia of the Alzheimer's type. II. Electron microscopy and pathogenic implications: effects of fixation on the morphology of the Alzheimer's abnormal filaments. Lab Invest 1989, 60:375–389
49. Crowther RA: Straight and paired helical filaments in Alzheimer disease have a common structural unit. Proc Natl Acad Sci USA, 1991, 88:2288–2292
50. Kosik KS, Greenberg SM: Tau proteins and Alzheimer disease. Alzheimer Disease. Edited by RD Terry, R Katzman, KL Bick. New York, Raven Press, 1994, pp 335–344
51. Metuzals J, Robitaille Y, Houghton S, Gauthier S, Kang CY, Leblanc R: Neuronal transformations in Alzheimer's disease. Cell Tissue Res 1988, 252:239–248
52. Crowther RA, Wischik CM: Image reconstruction of the Alzheimer paired helical filament. EMBO J 1985, 4:3661–3665
53. Crowther RA: Review: structural aspects of pathology in Alzheimer's disease. Biochim Biophys Acta 1991, 1096:1–9
54. Furcinitti PS, van Oostrum J, Burnett RM: Adenovirus polypeptide IX revealed as capsid cement by difference images from electron microscopy and crystallography. EMBO J 1989, 8:3563–3570
55. Tracz E, Dickson DW, Hainfeld JF, Ksiezak-Reding H: The ultrastructure of paired helical filaments with Nano-Van, a novel negative stain reagent. Int Conf EM 1994, 13:675–676
56. Paulus W, Selim M: Corticonigral degeneration with neuronal achromasia and basal neurofibrillary tangles. Acta Neuropathol (Berl) 1990, 81:89–94
57. Morishima-Kawashima M, Hasegawa M, Takio K, Suzuki M, Titani K, Ihara Y: Ubiquitin is conjugated with amino-terminally processed tau in paired helical filaments. Neuron 1993, 10:1151–1160
58. Yang LS, Ksiezak-Reding H: Ubiquitination of tau differs in paired helical filaments from Alzheimer's disease and corticobasal degeneration. Mol Biol Cell 1995, 6:37a